Clustered Wigner-crystal phases of cold polar molecules in arrays of one-dimensional tubes

Michael Knap,[1,2,*] Erez Berg,[2] Martin Ganahl,[1] and Eugene Demler[2]
[1]*Institute of Theoretical and Computational Physics, Graz University of Technology, 8010 Graz, Austria*
[2]*Department of Physics, Harvard University, Cambridge, Massachusetts 02138, USA*
(Received 23 December 2011; revised manuscript received 13 June 2012; published 1 August 2012)

We analyze theoretically polar molecules confined in planar arrays of one-dimensional tubes. In the classical limit, if the number of tubes is finite, new types of "clustered Wigner crystals" with increasingly many molecules per unit cell can be stabilized by tuning the in-plane angle between the dipolar moments and the tube direction. Quantum mechanically these phases melt into distinct "clustered Luttinger liquids." We calculate the phase diagram of the system and study the quantum melting of the clustered phases. We find that the requirements for exploring these phases are reachable in current experiments and discuss possible experimental signatures.

DOI: 10.1103/PhysRevB.86.064501 PACS number(s): 67.85.−d, 03.75.Hh, 05.30.−d, 34.20.−b

I. INTRODUCTION

Systems with competing long-range interactions often exhibit structures with emergent large length scales. Some examples include the formation of bubble and stripe domains in Langmuir-Blodgett films or in thin ferromagnetic layers,[1,2] and the chain formation of magnetic particles in three-dimensional ferrofluids.[3] Long-range dipolar interactions in a back-gated two-dimensional electron gas (2DEG) have been predicted[4,5] to lead to the existence of "microemulsion" phases intervening the Fermi liquid and the Wigner-crystal phase. Similar microemulsion phases may appear in 2DEGs subject to magnetic fields such that several Landau levels are occupied.[6–9]

Theoretically quantum emulsion phases are challenging to analyze since they involve structures at length scales ranging from the interparticle distance to mesoscopic scales. In contrast, the conventional tools of many-body physics are mostly geared toward two particle correlations, such as paired states, magnetism, and charge density wave. Experimentally quantum emulsion phases are not easy to probe since transport measurements can only provide indirect evidence about their existence. Realizing long-range interactions with systems of cold polar molecules[10–15] can allow us to explore emergent emulsion phases in a highly controllable setting. Moreover, in such systems few-body bound states,[16] trimer liquid phases,[17] and bound solitons[18] have been predicted.

Here we demonstrate that the anisotropic and long-range character of dipolar interactions leads to new types of clustered crystal phases which appear at *intermediate* values of the interaction strength. Quantum mechanically these phases melt into distinct "clustered Luttinger liquids" characterized by the decay of their density-density correlation functions. We calculate the phase diagram and study the quantum melting of the clustered phases when tuning the orientation of the dipoles. Our calculations indicate that the clustered phases can be explored under current experimental conditions.

II. EXPERIMENTAL SETUP

We consider a setup in which polar molecules are confined to n_T one-dimensional parallel tubes [see Fig. 1(a)], which can be realized by deep optical lattices.[19] The dipolar moments are aligned in the plane of the tubes at an angle ϕ with respect to the tube direction. The intertube distance δ is used as unit of length throughout this work.

The interaction energy between two molecules with dipolar moment $\mathbf{m}$ is

$$V(r\mathbf{e}_r) = \frac{\mu^2 - 3(\mathbf{m}\mathbf{e}_r)^2}{r^3}, \tag{1}$$

where $r\mathbf{e}_r$ is the intermolecule displacement and $\mathbf{m} = \mu(\cos\phi, \sin\phi, 0)^T$. For tilting angles below the critical angle $\phi_c = \arccos 1/\sqrt{3}$, the interaction between molecules in the same tube is attractive and the system is unstable. Thus, we focus on dipolar orientations $\pi/2 \geqslant \phi \geqslant \phi_c$ where the

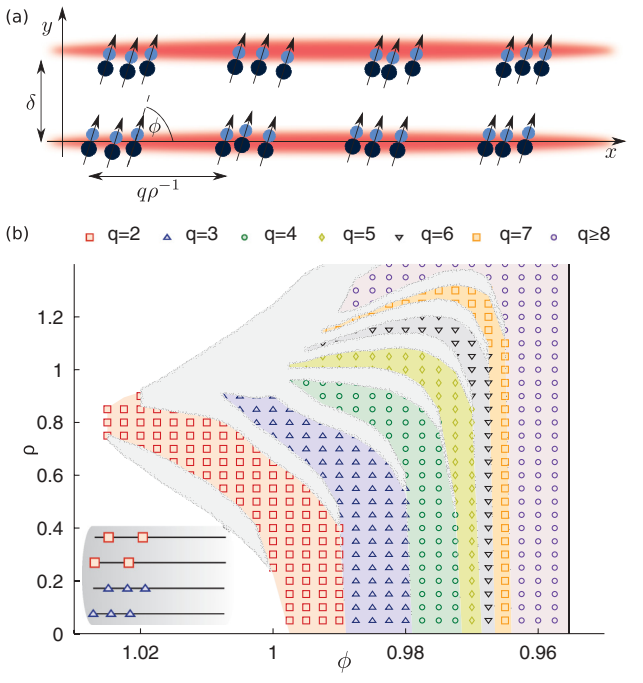

FIG. 1. (Color online) (a) Proposed setup to observe cluster formation of polar molecules. (b) The classical phase diagram for two tubes as a function of the tilting angle ϕ and the particle density ρ. Lobe shaped phases consisting of clusters with q particles per tube emerge. The phase separated regions are indicated by the shaded layer surrounded with speckles. Inset: Optimized cluster configuration in one unit cell for $\phi = 1.01$ (upper graph) and $\phi = 0.99$ (lower graph) at $\rho = 0.7$, corresponding to $q = 2$ and $q = 3$, respectively.

intratube interaction is repulsive. Yet, molecules in different tubes attract when their displacement along the tubes is not too large. It is precisely this interplay between attraction and repulsion which leads to the formation of clusters.

III. CLASSICAL LIMIT

We first discuss the emergence of mesoscopic structures in the classical limit ($\hbar \to 0$).

When the dipoles are oriented perpendicular to the tubes ($\phi = \pi/2$) the ground state is a Wigner crystal with n_T molecules per unit cell and periodicity ρ^{-1}, where ρ is the linear density of molecules. Upon tilting the direction of the dipoles toward the critical angle ϕ_c, phases with an increasingly complex unit cell are formed, before eventually becoming unstable to collapse at $\phi = \phi_c$. In these phases, the unit cell consist of q particles per tube forming a superlattice with periodicity $q\rho^{-1}$. For example, a phase with $n_T = 2$ and $q = 3$ is illustrated schematically in Fig. 1(a).

We derived the phase diagram as a function of the tilting angle ϕ and the density ρ by minimizing the classical ground-state energy with respect to the position of the molecules, allowing for arbitrary periodic structures with up to $q = 8$ molecules per unit cell in each tube. The phase diagram for $n_T = 2$ is shown in Fig. 1(b). At small densities we observe transitions to phases with monotonically increasing q when decreasing the tilt angle from $\pi/2$ toward ϕ_c. Phases of a fixed value of q have a lobelike structure, which bend with increasing density toward larger ϕ. Quite generally phases in Fig. 1(b) terminate by phase separated regions, indicated by a shaded layer surrounded with speckles. The phase separated regions are determined by the Maxwell construction which is applicable when the interfacial energy is positive.[4] It is possible that phases with $q > 8$, not captured by our present calculation, are favorable in some parts of the phase diagram. In particular, this is the case very close to $\phi = \phi_c$, where we find that $q = 8$ has the lowest energy.

The origin of the cluster formation can be easily understood by considering the case $\phi = \phi_c$. Then, the intratube repulsion is precisely zero. In order to maximize intertube attraction, it is favorable to form a single cluster with a macroscopic number of particles, corresponding to a $q \to \infty$ phase. As the angle is tuned toward ϕ_c, there must be either an infinite sequence of transitions to increasingly higher values of q, or a macroscopically phase separated region.[20]

Next we discuss systems with more than two tubes. Results for $n_T = 3$, 4, and 8 tubes are shown in Fig. 2. The phase diagrams for $n_T > 2$ have a similar lobe structure as in the $n_T = 2$ case. The main difference is that with increasing number of tubes the lobes extend to higher values of the tilting angle ϕ. Thus, clustered phases might be easier to observe in systems with a larger number of tubes. As in the $n_T = 2$ case, phase separated regions appear between phases of different q.

A two-dimensional system which consists of an infinite number of tubes with dipoles aligned in the plane exhibits similar physics: the $q = 1$ Wigner-crystal phase becomes locally unstable for $\phi > \phi_c$. However, in this case, trial configurations with an increasing q have monotonically lower energy (we have tried structures with up to $q = 128$), indicating that the ground state may be phase separated. In the low-density limit, the dipoles form infinitely long strings, which are mutually attractive[20] and thus one can show that the system is unstable to macroscopic phase separation. Note that, for in-plane dipoles, the (logarithmically divergent) surface energy is *positive*,[20] therefore macroscopic phase separation is possible (unlike the out-of-plane case[4]).

IV. QUANTUM MECHANICAL ANALYSIS

In quantum mechanical systems with continuous translational symmetry, true long-range crystalline order appears only in two dimensions or higher, even at zero temperature. In one-dimensional systems, the density-density correlations decay for large distances as a power law. Nevertheless, one can expect that upon melting the clustered Wigner-crystal phases by quantum fluctuations, these phases will remain distinguishable by the nature of their quasi-long-range correlations. We term the resulting phases clustered Luttinger liquids.

In a clustered Luttinger liquid phase, the slowest-decaying component of the density-density correlations has a spatial period of $\lambda = q\rho^{-1}$. In a bosonized description, the fundamental harmonic of the density operator is therefore of the form $\cos[2\pi(x + x_0)\rho/q]$, where x_0 is a uniform shift of the crystalline configuration. In terms of the "counting field" $\phi(x)$[24] defined relative to the crystalline configuration we obtain for the bosonized density

$$\rho(x) = \rho - \frac{1}{\pi}\nabla\phi(x) + \rho\cos\left[\frac{2\pi\rho x}{q} + \frac{2\phi(x)}{q}\right] + \ldots,$$

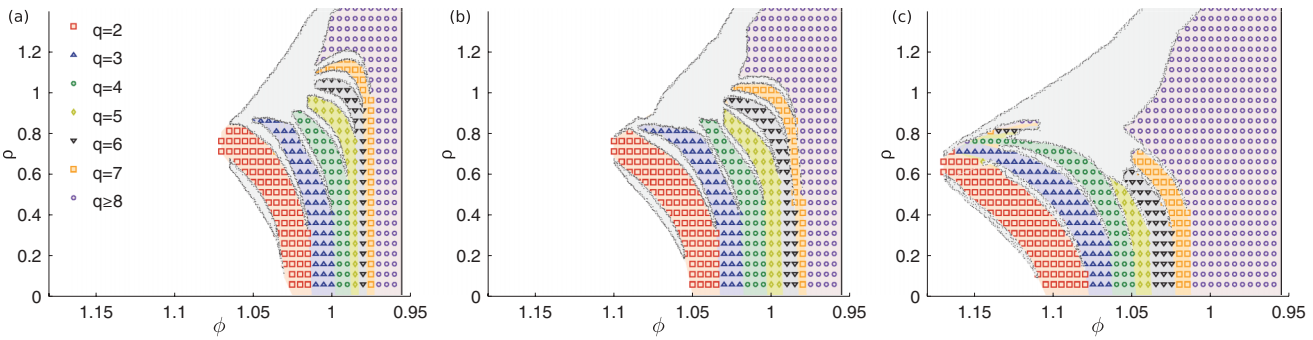

FIG. 2. (Color online) Phase diagram in the tilting angle ϕ and the particle density ρ plane for (a) $n_T = 3$, (b) $n_T = 4$, and (c) $n_T = 8$ tubes. The phase separation regions are indicated by shaded layers.

where the dots represent higher harmonics. The factor q^{-1} present in the cosine alters the power law with which the density correlations decays:

$$\langle \rho(x)\rho(0)\rangle = \rho^2 - \frac{K}{2\pi^2}\frac{1}{x^2} + \frac{\rho^2}{2}\cos\frac{2\pi\rho x}{q}\left(\frac{\alpha}{x}\right)^{\frac{2K}{q^2}}. \quad (2)$$

Here K is the Luttinger parameter. Microscopic considerations[20] suggest that $K \propto q$. Therefore, the exponent with which the density-density correlation function decays is proportional to $1/q$. Phases with larger q thus have a slower decay of the density-density correlation function, and are increasingly "classical" in nature.

In order to make quantitative predictions about the phase diagram in the presence of quantum fluctuations, we have investigated a system of two tubes numerically by means of density matrix renormalization group (DMRG)[26,27] simulations. To this end, we introduce the lattice Hamiltonian

$$\hat{H} = -t\sum_{\alpha,i}[c^\dagger_{\alpha,i}c_{\alpha,i+1} + c^\dagger_{\alpha,i+1}c_{\alpha,i}] + \frac{\mu^2}{\delta^3}{\sum_{i,j,\alpha,\beta}}' V_d[(i-j)a/\delta, \alpha-\beta]\hat{n}_{\alpha,i}\hat{n}_{\beta,j}, \quad (3)$$

where $c_{\alpha,i}$ ($c^\dagger_{\alpha,i}$) destroys (creates) a particle at site i of tube $\alpha = 1, 2$, and $\hat{n}_{\alpha,i} = c^\dagger_{\alpha,i}c_{\alpha,i}$ counts the number of particles. Due to the strong on-site repulsion we treat the particles as hard core, and therefore for the quantities we compute here (e.g., density distributions and ground-state energies) it does not matter whether the particles are bosons or fermions. The discrete Hamiltonian can represent a continuous system by taking the lattice spacing $a \to 0$ while keeping the product $ta^2 = 1/(2m)$ constant, where t is the hopping strength and m is the mass of the particles in the continuum. The primed sum indicates that the singular contribution where $i = j$ and simultaneously $\alpha = \beta$ is omitted. The dipolar energy $V_d(x, y)$ is given by Eq. (1) with $\mathbf{r} = (x, y)^T$.

It is convenient to introduce the dimensionless quantity γ, which is the ratio between the typical dipolar interaction energy $E_{\rm dip}$ and the typical kinetic energy $E_{\rm kin}$. These energies can be estimated as $E_{\rm dip} \sim \mu^2\rho^3$ and $E_{\rm kin} \sim \rho^2/m$, respectively, and thus $\gamma \sim \mu^2\rho m$. In the limit of strong interactions, $\gamma \gg 1$, the system is expected to be essentially classical, and the phase diagram is expected to be similar to that of Fig. 1 with the Wigner-crystalline phases replaced by clustered Luttinger liquids. Conversely, for $\gamma \ll 1$, quantum fluctuations dominate, and we expect only the $q = 1$ phase to survive.

The particle density $\rho(x)$ evaluated with DMRG for the Hamiltonian (3) exhibits clear signatures of clustered phases, see Fig. 3. We consider a system of finite length $L = 24\delta$ with open boundary conditions and particle density $\rho = 0.5\delta^{-1}$ and dipolar strength $\gamma = 50$. The lattice constant is $a = \delta/4$; no significant change in the results was observed when a was decreased to $\delta/6$. Since the reflection symmetry about a plane perpendicular to the tube is broken for any tilting angle except $\phi = \pi/2$, the density of the upper ρ_u and the lower ρ_l tube are slightly shifted. Additionally, we observe that the height of the peaks in the density decreases toward the trap center, consistent with quasi-long-range order. Remarkably, the rate of the decay decreases strongly with increasing q, as expected from the Luttinger liquid analysis [Eq. (2)].

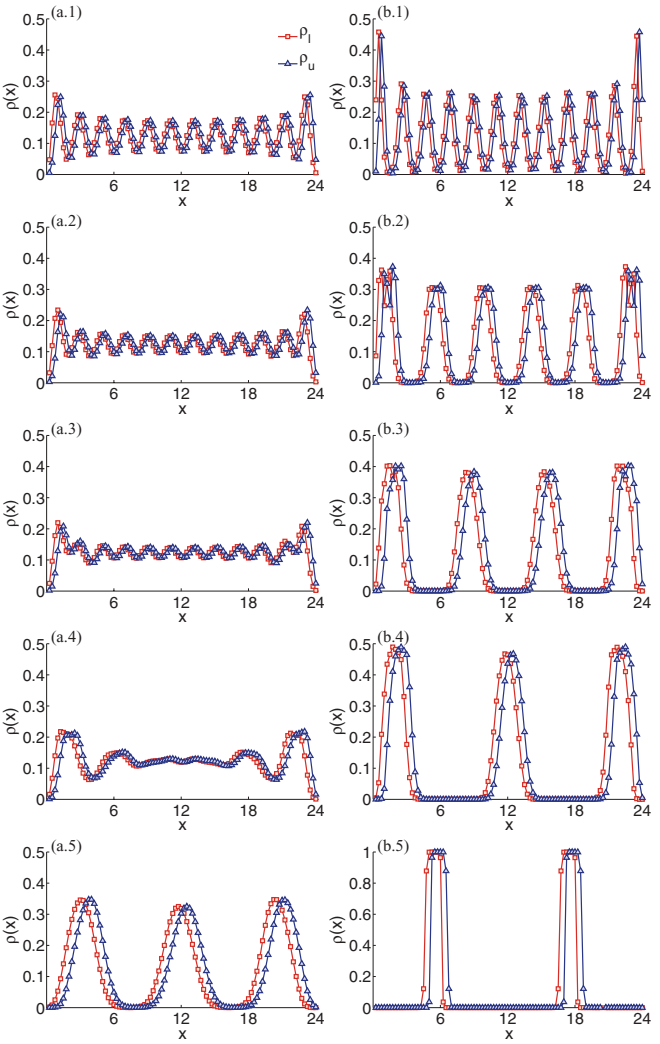

FIG. 3. (Color online) Particle density $\rho(x)$ in the lower (red squares) and the upper (blue triangles) tube for dipolar strength $\gamma = 8$, left column, and $\gamma = 50$, right column, for a system of length $L = 24\delta$, density $\rho = 0.5\delta^{-1}$, and lattice spacing $a = \delta/4$. From top to bottom the tilt angle takes the values $\phi = \{1.02, 0.99, 0.98, 0.97, 0.96\}$. For $\gamma = 50$ pronounced clusters with $q = \{1, 2, 3, 4, 6\}$ are found. The data is obtained by DMRG for systems with open boundary conditions.

The complete quantum phase diagram for the two tube system as a function of the tilting angle ϕ and the ratio between kinetic and interaction energy $1/\gamma$ is shown in Fig. 4. For $1/\gamma = 0$, the results were obtained by classical minimization of the interaction energy. The DMRG simulations are used to extend the results to $1/\gamma > 0$. The phases are determined from the density distribution by calculating the number of particles localized within one cluster. The clustered Luttinger liquid phases with $q > 1$ extend to considerably large values of $1/\gamma$, making the realization of

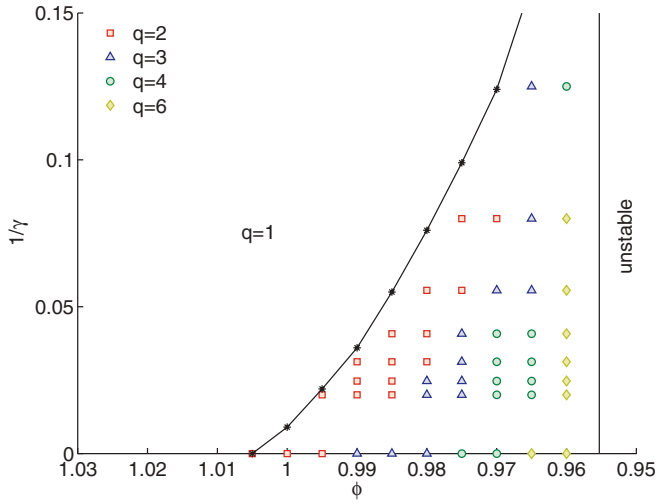

FIG. 4. (Color online) Quantum phase diagram for a two tube system of length $L = 24\delta$, density $\rho = 0.5\delta^{-1}$, and lattice spacing $a = \delta/4$, as a function of the tilting angle ϕ and the ratio between the kinetic and the interaction energy $1/\gamma$. Right of the asterisks, connected by lines, cluster formation can be observed. To the left of this line, the ground state is a $q = 1$ Luttinger liquid.

clustered phases feasible in experiments with cold dipolar molecules.

V. EXPERIMENTAL IMPLICATIONS

For typical densities of $\rho = 10^4\,\mathrm{cm}^{-1}$, $\gamma \sim \{0.7, 3.3, 6.8, 49.4, 63.3\}$ can be achieved in experiments with KRb, RbCs, NaK, NaCs, and LiCs, respectively. (See Ref. 20 for details on this calculation.)

The density regime, which is most favorable for observing clustered phases, is $\rho \sim 0.5\delta^{-1} - \delta^{-1}$. For $\rho \sim 10^4\,\mathrm{cm}^{-1}$, this corresponds to an intertube separation of $\delta \sim 5 \times 10^{-5}$ cm, easily attainable using an optical potential created by a laser with wavelength $\sim 1\ \mu$m.

NaCs and LiCs are thus the most promising candidates to realize clustered phases, due to their large dipolar moments. In order to make the clustered phases more robust, one can add a shallow periodic potential along the tubes. Such a periodic potential quenches the kinetic energy, thus increasing the effective value of γ. As a consequence, cluster formation arises at a much weaker dipolar moment also attainable by KRb.

Other effects that can be important for experiments are (i) the incommensurability of the particle number with the cluster size, (ii) the shallow trap potential along the tube direction, (iii) the strong but finite transverse confinement, (iv) quantum fluctuations in the orientation of the dipoles, and (v) finite temperature effects. Cluster formation is extremely stable with respect to (i) and (ii).[20] Incommensurability leads to a slight rearrangement of clusters and the consequence of the shallow trap along the tubes is merely that the distance between the clusters is reduced. One-dimensional tubes are realized by strong transverse confinement potentials (iii). Therefore, we consider the interactions computed for molecules with transverse wave functions, corresponding to a parabolic confinement, and compare them to the bare, one-dimensional interactions. The renormalization of the interactions due to the transverse confinement can be evaluated from a multipole expansion yielding $\Delta E^{\perp}_{\mathrm{dip}}/E_{\mathrm{dip}} \lesssim \sigma^2/\delta^2$, where σ is the spread of the wave function in transverse direction.[20] Under standard experimental conditions $\sigma \sim 25$ nm and thus $\Delta E^{\perp}_{\mathrm{dip}}/E_{\mathrm{dip}} \lesssim 0.0025$. This ratio has to be compared with the relative energy difference between the clustered $q > 1$ and the uniform $q = 1$ phase, which typically is $0.2 - 0.5 \gg \Delta E^{\perp}_{\mathrm{dip}}/E_{\mathrm{dip}}$. Therefore, the renormalization of the interaction energy due to the finite strength of the transverse confinement is no obstacle for the observability of the clustered phases. The quantum fluctuations of the dipoles around the orientation of the electric field (iv) renormalize the dipolar potential by $\Delta E^{e}_{\mathrm{dip}}/E_{\mathrm{dip}} \lesssim R_e/\delta \sim 0.001$, where R_e is the bond length of the molecule. Thus, this effect is also small. The temperature scale (v) below which we expect strong tendency toward cluster formation, is proportional to the dipolar energy E_{dip}. In units of the Fermi temperature $T_F \sim E_{\mathrm{kin}}$ the crossover temperature is $T_{\mathrm{cross}} = \alpha\gamma$, where the proportionality constant α can be estimated from the relative energy difference of the uniform and the clustered phases, that is, $\alpha \sim 0.2$–0.5. Depending on the molecule[20] the crossover temperature is $T_{\mathrm{cross}} \gtrsim T_F$.

VI. CONCLUSIONS AND OUTLOOK

In summary, the formation of clustered phases of polar molecules is a distinct consequence of the long-range and anisotropic nature of their interactions. We find that the clustered phases can be explored under current experimental conditions. A variety of techniques can be employed to observe the clustered phases, including elastic light scattering,[33] noise correlations in time-of-flight images,[34] and optical quantum nondemolition detection.[16,35] Cluster formation should also contribute additional dissociation resonances in lattice modulation experiments[36] and rf spectroscopy.[37–39]

A particular exciting direction for future research is to study excitations in this system. For the simple $q = 1$ phase, the unit cell consists of a single particle per tube and thus only the acoustic mode exists. However, in clustered crystal phases with $q > 1$ optical branches should also exist in the excitation spectra.

ACKNOWLEDGMENTS

We are grateful to E. G. Dalla Torre for insightful discussions about the Luttinger liquid analysis. M.K. wants to thank W. von der Linden and E. Arrigoni for fruitful discussions. The authors acknowledge support from Harvard-MIT CUA, the NSF Grants No. DMR-07-05472 and No.DMR-07-57145, the DARPA OLE program, AFOSR Quantum Simulation MURI, AFOSR MURI on Ultracold Molecules, the Austrian Science Fund (FWF) under Project No. P18551-N16 (M.K.) and within the SFB ViCoM (F41) (M.G.), as well as the Austrian Marshall Plan Foundation (M.K.). Calculations have been partly performed on the iCluster of Graz University of Technology.

*michael.knap@tugraz.at

[1] K. O. Ng and D. Vanderbilt, Phys. Rev. B **52**, 2177 (1995).

[2] V. I. Marchenko, Zh. Eksp. Teor. Fiz. **90**, 2241 (1986).

[3] R. E. Rosenweig, *Ferrohydrodynamics* (Cambridge University Press, Cambridge, 1985).

[4] B. Spivak and S. A. Kivelson, Phys. Rev. B **70**, 155114 (2004).

[5] B. Spivak, S. V. Kravchenko, S. A. Kivelson, and X. P. A. Gao, Rev. Mod. Phys. **82**, 1743 (2010).

[6] A. A. Koulakov, M. M. Fogler, and B. I. Shklovskii, Phys. Rev. Lett. **76**, 499 (1996).

[7] R. Moessner and J. T. Chalker, Phys. Rev. B **54**, 5006 (1996).

[8] M. M. Fogler, in *High Magnetic Fields: Applications in Condensed Matter Physics and Spectroscopy*, 1st ed. (Springer, Berlin, 2002), pp. 98–138.

[9] J. P. Eisenstein, K. B. Cooper, L. N. Pfeiffer, and K. W. West, Phys. Rev. Lett. **88**, 076801 (2002).

[10] L. Santos, G. V. Shlyapnikov, P. Zoller, and M. Lewenstein, Phys. Rev. Lett. **85**, 1791 (2000).

[11] M. A. Baranov, M. S. Marenko, V. S. Rychkov, and G. V. Shlyapnikov, Phys. Rev. A **66**, 013606 (2002).

[12] J. Doyle, B. Friedrich, R. V. Krems, and F. Masnou-Seeuws, Eur. Phys. J. D **31**, 149 (2004).

[13] M. Baranov, Phys. Rep. **464**, 71 (2008).

[14] L. D. Carr, D. DeMille, R. V. Krems, and J. Ye, New J. Phys. **11**, 055049 (2009).

[15] T. Lahaye, C. Menotti, L. Santos, M. Lewenstein, and T. Pfau, Rep. Prog. Phys. **72**, 126401 (2009).

[16] B. Wunsch, N. T. Zinner, I. B. Mekhov, S. J. Huang, D. W. Wang, and E. Demler, Phys. Rev. Lett. **107**, 073201 (2011).

[17] M. Dalmonte, P. Zoller, and G. Pupillo, Phys. Rev. Lett. **107**, 163202 (2011).

[18] M. Bauer and M. M. Parish, Phys. Rev. Lett. **108**, 255302 (2012).

[19] A. Chotia, B. Neyenhuis, S. A. Moses, B. Yan, J. P. Covey, M. Foss-Feig, A. M. Rey, D. S. Jin, and J. Ye, Phys. Rev. Lett. **108**, 080405 (2012).

[20] See Supplemental Material at http://link.aps.org/supplemental/10.1103/PhysRevB.86.064501 for details on the experimental feasibility, the classical limit, and the quantum mechanical analysis.

[21] P. P. Ewald, Ann. Phys. **369**, 253 (1921).

[22] U. Essmann, L. Perera, M. L. Berkowitz, T. Darden, H. Lee, and L. G. Pedersen, J. Chem. Phys. **103**, 8577 (1995).

[23] A. Grzybowski, E. Gwóźdź, and A. Bródka, Phys. Rev. B **61**, 6706 (2000).

[24] T. Giamarchi, *Quantum Physics in One Dimension* (Oxford University Press, New York, 2004).

[25] C. Kollath, J. S. Meyer, and T. Giamarchi, Phys. Rev. Lett. **100**, 130403 (2008).

[26] S. R. White, Phys. Rev. Lett. **69**, 2863 (1992).

[27] U. Schollwöck, Rev. Mod. Phys. **77**, 259 (2005).

[28] K. Ni, S. Ospelkaus, M. H. G. de Miranda, A. Pe'er, B. Neyenhuis, J. J. Zirbel, S. Kotochigova, P. S. Julienne, D. S. Jin, and J. Ye, Science **322**, 231 (2008).

[29] M. Debatin, T. Takekoshi, R. Rameshan, L. Reichsöllner, F. Ferlaino, R. Grimm, R. Vexiau, N. Bouloufa, O. Dulieu, and H. Nägerl, Phys. Chem. Chem. Phys. **13**, 18926 (2011).

[30] J. W. Park, C. Wu, I. Santiago, T. G. Tiecke, P. Ahmadi, and M. W. Zwierlein, Phys. Rev. A **85**, 051602(R) (2012).

[31] C. Haimberger, J. Kleinert, O. Dulieu, and N. P. Bigelow, J. Phys. B **39**, S957 (2006).

[32] J. Deiglmayr, M. Repp, A. Grochola, K. Mörtlbauer, C. Glück, O. Dulieu, J. Lange, R. Wester, and M. Weidemüller, Faraday Discuss. **142**, 335 (2009).

[33] C. A. Müller, T. Jonckheere, C. Miniatura, and D. Delande, Phys. Rev. A **64**, 053804 (2001).

[34] E. Altman, E. Demler, and M. D. Lukin, Phys. Rev. A **70**, 013603 (2004).

[35] N. T. Zinner, B. Wunsch, I. B. Mekhov, S. J. Huang, D. W. Wang, and E. Demler, Phys. Rev. A **84**, 063606 (2011).

[36] T. Stöferle, H. Moritz, C. Schori, M. Köhl, and T. Esslinger, Phys. Rev. Lett. **92**, 130403 (2004).

[37] C. A. Regal and D. S. Jin, Phys. Rev. Lett. **90**, 230404 (2003).

[38] S. Gupta, Z. Hadzibabic, M. W. Zwierlein, C. A. Stan, K. Dieckmann, C. H. Schunck, E. G. M. van Kempen, B. J. Verhaar, and W. Ketterle, Science **300**, 1723 (2003).

[39] C. A. Regal, C. Ticknor, J. L. Bohn, and D. S. Jin, Nature (London) **424**, 47 (2003).